Velocity measurement in an arterial blood filter using the laser Doppler anemometry technique

by

R. Huebner[(1)], E.P. Tomasini[(2)], N. Paone[(3)], P. Castellini[(4)], M. Pinotti[(5)] and G.A.C. França[(6)]

Pontíficia Universidade Católica de Minas Gerais [(1)]

Instituto Politécnico – Departamento de Engenharia Mecânica

Av. Dom José Gaspar, 500 – Coração Eucarístico – Belo Horizonte – MG – CEP – 30535-610; Brasil

Università degli Studi di Ancona[(2), (3), (4)]

Dipartimento di Meccanica

Via Brecce Bianche, 60131 – Ancona; Italia

Universidade Federal de Minas Gerais [(5), (6)]

Departamento de Engenharia Mecânica

Av. Antônio Carlos, 6627 – Pampulha – Belo Horizonte – MG – CEP 31270-901; Brasil

[(1)]E-Mail: rudolf@pucminas.br

[(2)]E-Mail: tomasini@mehp1.unian.it

[(3)]E-Mail: nicola@mehp1.unian.it

[(4)]E-Mail: cast@mehp1.unian.it

[(5)]E-Mail: pinotti@demec.ufmg.br

[(6)]E-Mail: franca@demec.ufmg.br

ABSTRACT

Damage to red blood cells can be induced chemically, by osmosis or mechanically. The fluid mechanical effect can be related to the device design, its surface characteristics and to the degree of flow disturbance or turbulence caused by the device. Is generally accepted that the presence of high turbulent shear stresses generated in the flow fields of artificial devices are partially responsible for the levels of red blood cells destruction, or hemolysis. Investigating the effect of turbulent shear stress on hemolysis is of prime importance to research work related to artificial devices. Hemolysis is a function of the shear stresses magnitude acting on blood cells and their exposure time to the shear stresses. The present work presents the use of two techniques used to study the flow in an arterial blood filter. The general structure of the flow field was analyzed using the dye injection technique. A laser Doppler anemometer was used to measure two orthogonal velocity components and their fluctuations, which were used to evaluate turbulent stresses.

1. INTRODUCTION

Nowadays cardiopulmonary bypass (CPB) with extracorporeal blood oxygenation is a very common practice. Microembolization occurs during CPB due to the presence of bubbles air, thrombi, platelet aggregates and pieces of plastic into the arterial line as cited by Waaben *et al*. (1994). Microemboli can cause organ dysfunction, especially in the brain, liver, lung and kidney. The use of a blood filter in the arterial line of the extracorporeal circuit has been one of the proposed methods to retain microemboli thus avoiding organ dysfunction.

Blood flow through artificial devices (heart valves, blood pumps, oxygenators and filters) is associated with thrombus formation and hemolysis (red blood cell damage). Hemolysis is one of the most difficult problems encountered in extracorporeal circulation. The mechanism that causes red blood cell damage is not completely clear, namely the relationship between hemolysis and blood flow behaviour. Flow behaviour can be considered in terms of pressure levels, turbulence intensity, flow acceleration and stagnation. Hemolysis has been associated with elevated Reynolds stresses produced by turbulent flows.

Red blood cells damage can be induced at moderate shear stress in the presence of a foreign surface, as shown by Sutera and Mehrjardi (1975). Sutera (1977) has shown that prolonged exposure to turbulent shear stresses as low as 150 N/m^2 can produce lysis of red blood cells. Sallam and Hwang (1984) have shown that incipient hemolysis begins at Reynolds stresses of about 400 N/m^2. The resistance of red blood cells to shearing forces is higher than was assumed, reaching a threshold of 500 N/m^2 for 1 s of exposure (Paul *et al*., 1999).

In this work the flow structure in an arterial blood filter is analysed. Some regions of the filter were studied using the laser Doppler velocimetry technique and velocity profiles, their fluctuations and turbulent stresses are presented. The dye injection technique was used in order to analyse the general flow structure in the blood filter.

2. EXPERIMENTAL METHOD and PROCEDURES

2.1 The Blood Filter

The filter is used in cardiopulmonary bypass procedures. The body filter is made of acrylic and a polyester screen is used in the filtering element. The filtering element has a porosity of 40 μm. The filter inlet and outlet connectors have a diameter of 9,5 mm and are made of reinforced acrylic. The filter has a volume of about 280 ml, is projected to be used in adult patients and can be operated with a maximum flow rate of 6 litres per minute. The filter has a bypass line that can be used in situations where the filtering element pores are closed and another line is used to eliminate air trapped by the filter. Figure 1 shows a schematic view of the filter, its elements and how it works. In figure 1, blue arrows are used to indicate unfiltered blood while red arrows indicate filtered blood.

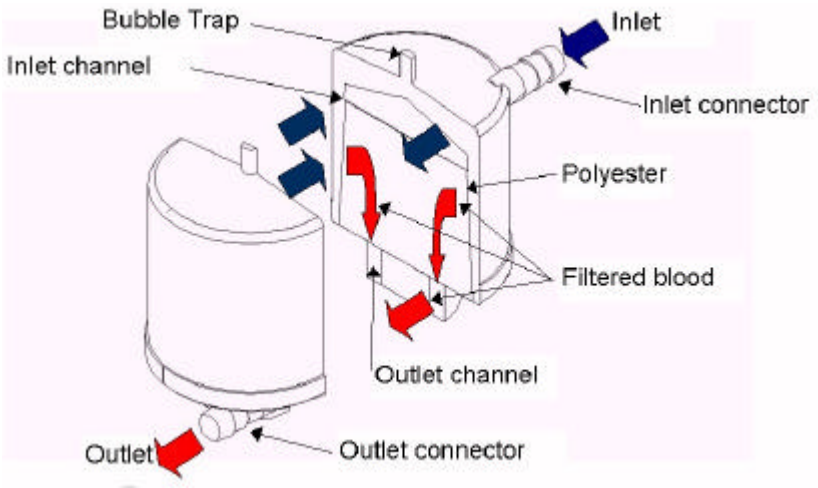

Fig. 1. Schematic view of the filter

Blood flows through the inlet connector, located at the upper part of the filter, and describes a descending helical movement while it flows along the inlet channel. During this helical movement the blood flows through the filtering element, polyester, reaches the outlet channel and flows in direction of the outlet connector, located at the bottom of the filter.

2.2 The Test Bench

A test bench was assembled in order to reproduce the flow condition observed during a cardiopulmonary bypass. Figure 2 depicts schematically the test circuit.

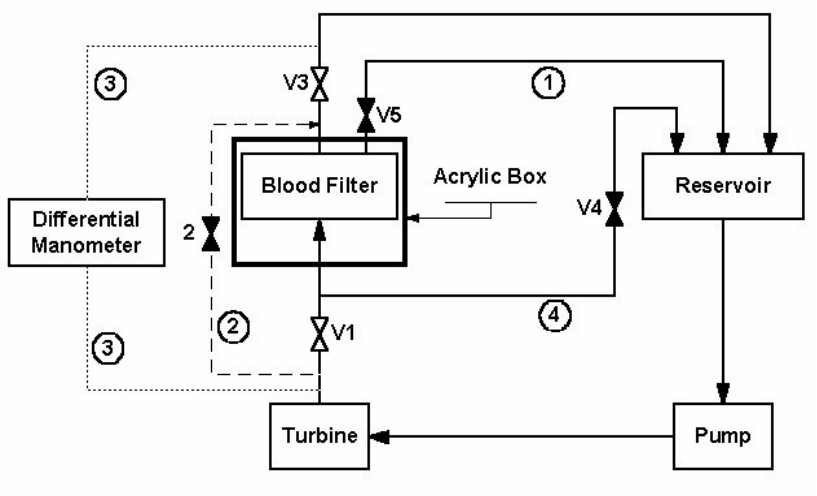

Fig. 2. Schematic view of the test circuit.

Working fluid was pumped, using a blood pump (Spiral pump), through the turbine and blood filter returning to the circuit reservoir. Line 1 represents the bubble trap and was used during the circuit filling up. During the LDA measurements many particles, necessary due to the LDA working principle, were captured by the filtering element and Lines 2 and 4 were used together to clean the filter using a retrograde flow. Pressure drop across the filter was monitored by a differential manometer, indicated by the lines 3. Flow rate was monitored by a turbine flowmeter (ITT Barton, model 7182) and the pump rotating speed was controlled changing the excitation voltage of a brushless motor. All elements of the circuit were connected using PVC flexible tubes.

Fig. 3 Some elements of the test circuit. Left the blood pump and right the turbine flowmeter.

A prismatic acrylic box was used as optical window to minimise optical distortions. During the LDA measurements and flow visualisation tests the filter was placed inside this prismatic box filled with water. The flow rate used in the LDA tests was 4.5 liters per minute which is an accordance with the values used during a cardiopulmonary bypass. The flow was seeded with Al_2O_3 particles with a mean measured diameter of 48 μm. Water was used during the visualisation tests

using dye injection and the flow rate was estimated using Reynolds similitude between water and the water-glycerine solution.

2.3 Laser Doppler Anemometry

A two-component fiber optic laser Doppler anemometer (DANTEC) was used to measure the axial and tangential velocity components. In this system a 4 W argon-ion laser was coupled to a fiber drive unit which allowed for a colour separation of the primary beam. The resulting green (514.5 nm wavelength) and blue (488 nm wavelength) beams were used for the velocity measurements. A 160 mm focal length lens was coupled to the LDA probe to produce an ellipsoidal measurement volume with a maximum length, in air, of 0.658 mm and a diameter of 0,078 mm. The Doppler signal were processed with fast Fourier signal analyser and a commercial software (Burstware) was used to acquire data and to control the signal analysers and the photomultiplier. Approximately 3000 measurements were acquired for each spatial location. LDA measurements were done at four different planes labelled N, S, E and O and each plane was divided in eight levels. A coordinate system was adopted in order to perform the measurements. The system is oriented in such a way that x axis is directed radially, y axis axially and z axis is tangential to the filter. Z axis is horizontally directed and always parallel to the LDA probe surface. Figure 4 shows the measurement planes and the coordinate system used during the LDA measurements. The first level was located 13 mm above the intersection of the bottom piece with the lateral piece of the filter and the next level was placed 5 mm above the previous. The tangential velocity (U) is positive in the negative sense of the z axis while the axial velocity (V) is positive following the y axis sense.

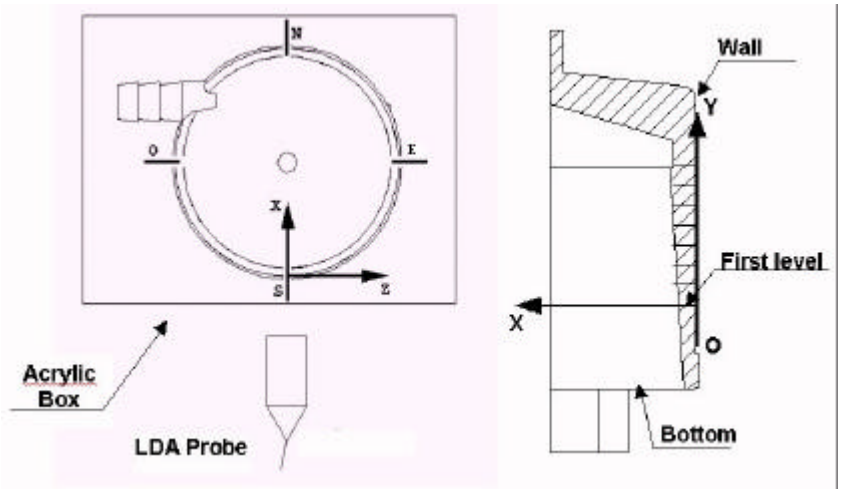

Fig. 4. Coordinate systems and measurement planes.

Figure 5 shows the test circuit and the filter inside the acrylic box. Left we can see the blood pump and its controller, the frequency counter (HAMEG, model 8012-3) used with the flowmeter, the reservoir, the LDA probe, the acrylic box and the filter inside it. Right we have a detail of the filter inside the box, the LDA probe e the light reflected by the filter element (polyester).

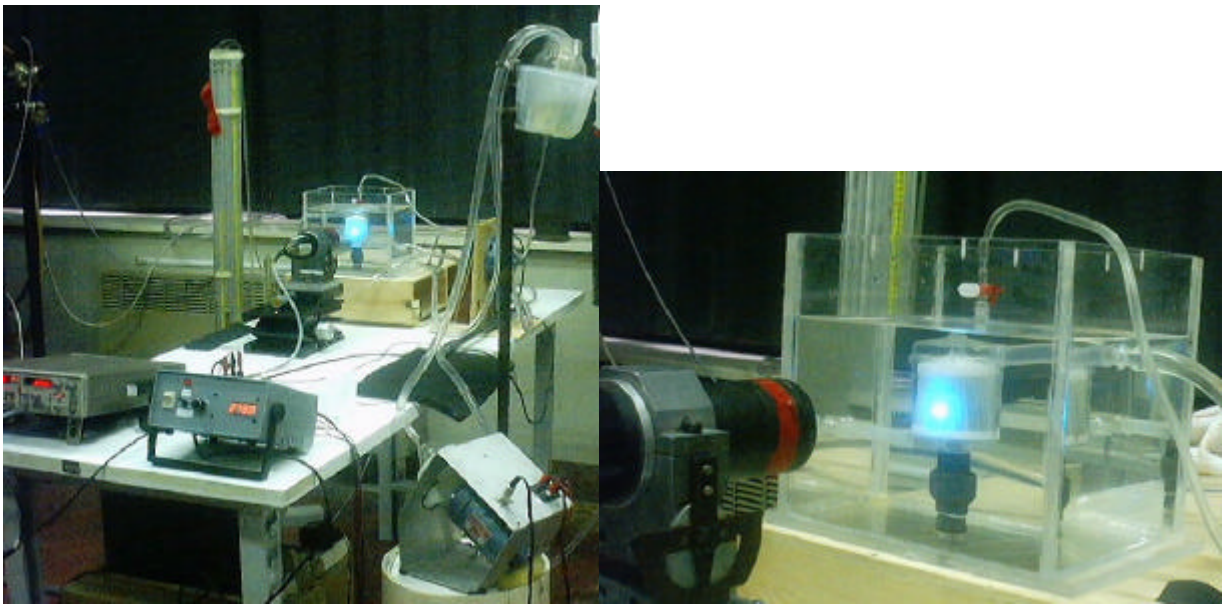

Fig. 5. The test circuit and the filter inside the acrylic box filled with water..

The working fluid was a combination of 40%, in mass, of glycerine with 60% of water. This working fluid was chosen because it matches the blood transport properties. At 25°C, the blood analogue fluid has a density of 1.09 g/cm^3 and absolute viscosity of 3.18 mPa.s. One problem associated with this working fluid when using a optical measurement technique is the refraction index. The measured refraction index of the solution was 1.383 which is lower than 1.49, the refractive index of the filter wall. This difference implies in a displacement of the LDA measurement volume due to the refraction of the laser beams. An equation that describes the position of the measurement volume inside the filter was developed using Snell´s law. Figure 6 shows the refraction of two laser beams crossing to materials with different refraction index. The beams should intercepted at O but they intercepted at O´ due to the difference between n_1 and n_2, the materials refraction indexes.

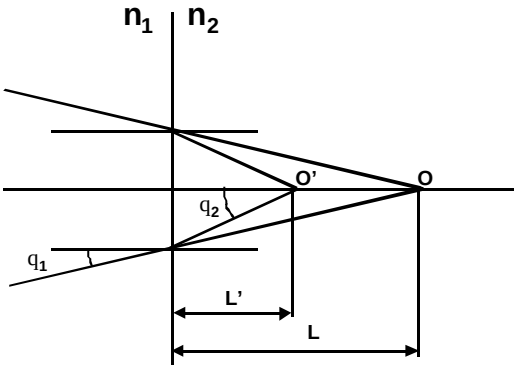

Fig. 6. Laser beams crossing two different materials.

Snell´s law is used to evaluate the correct position of the measurement volume (Dybbs and Edwards, 1987).

$$\frac{L'}{L} = \frac{\mathrm{Tan}\, q_1}{\mathrm{Tan}\, q_2} \tag{1}$$

The instantaneous velocities ($\tilde{u}_n$ and $\tilde{v}_n$), measured by the LDA, can be separated into mean components (U and V) and fluctuating components (u_n e v_n). Mean velocities can be evaluated as

$$\overline{U} = \frac{1}{N}\sum_{1}^{N} \tilde{u}_n \tag{2}$$

and

$$\overline{V} = \frac{1}{N}\sum_{1}^{N} \tilde{v}_n \,, \tag{3}$$

where N is the number of collected samples. The fluctuating components are estimated using equations (4) and (5).

$$u_n = \tilde{u}_n - \overline{U} \tag{4}$$

and

$$v_n = \tilde{v}_n - \overline{V} \,. \tag{5}$$

The gate-time averaging technique was adopted in order to remove the "velocity bias" which, would lead to the overestimation of the velocity. Techniques for determining Reynolds stresses in stationary flows from LDA measurements are well established (Baldwin et all, 1993). Reynolds normal stresses ($\overline{\rho uu}$ e $\overline{\rho vv}$) and shear stress ($\overline{\rho uv}$) are determined by the following equations.

$$\overline{\rho uu} = \frac{1}{N}\sum \rho u_n^2 \,, \tag{6}$$

$$\overline{\rho vv} = \frac{1}{N}\sum \rho v_n^2 \,, \tag{7}$$

and

$$\overline{\rho uv} = \frac{1}{N}\sum_{1}^{N} \rho u_n v_n \,. \tag{8}$$

Normal and shear stresses were used to evaluate principal stresses. Principal stresses were estimated using the equation proposed by Higdon et all (1985)

$$\overline{\sigma}_{max,min} = \frac{\overline{\rho uu} + \overline{\rho vv}}{2} \pm \sqrt{\left(\frac{\overline{\rho uu} - \overline{\rho vv}}{2}\right)^2 + \overline{\rho uv}^2} \,, \tag{9}$$

and the maximum shear stress can then be obtained from the principal stresses as

$$\tau_{max} = \frac{1}{2}\left(\sigma_{max} - \sigma_{min}\right) \tag{10}$$

The turbulent kinetic energy was evaluated using the following equation.

$$ECT = \frac{u_n^2 + v_n^2}{2} \tag{11}$$

2.4 Flow Visualisation

Flow visualization was performed using the same test bench described before. Dye was injected, using a needle, through the inlet connector or through one of the eight orifices made at the upper part of the filter. At each orifice the dye was injected at three different levels. Figure 7 shows the injection points and levels. It must be pointed out that the nomenclature used to label the measurement planes was adopted to the injection points. Visualization was performed using a WEB camera placed normal to the filter wall in the region where the needle was placed.

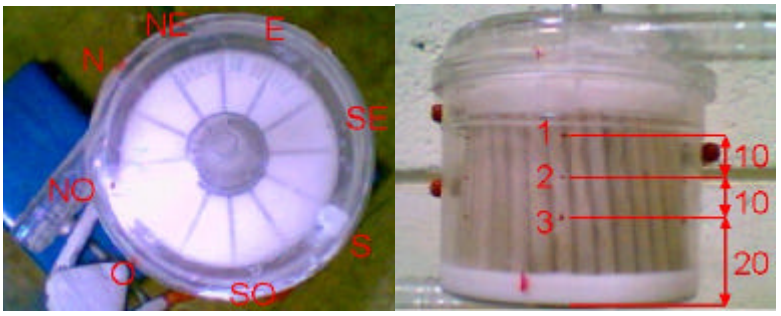

Fig. 7. Injection points and levels

Water, at 25°C, was used as working fluid and Reynolds similitude was used to evaluate the water flow rate. The characteristic length used in the Reynolds number evaluation was the diameter of the inlet connector.

$$Re_{water} = Re_{sol.40\%} \tag{12}$$

and so

$$\frac{r_{water} V_{water} D_{filter}}{m_{water}} = \frac{r_{sol.40\%} V_{sol.40\%} D_{filter}}{m_{sol.40\%}}. \tag{13}$$

Water flow rate can be expressed in terms of water-glycerine flow rate and kinematics viscosity as

$$Q_{water} = \frac{n_{water}}{n_{sol.40\%}} Q_{sol.40\%} = \frac{0{,}857}{2{,}898} 4{,}5 = 1{,}33 \tag{14}$$

The flow rate used was 1,33 l/min. The similitude asserts that the flow pattern observed using water is the same that using the solution of water and glycerin.

3. RESULTS AND DISCUSSION

3.1 Flow Visualisation

Figure 8 shows the flow visualization, at the upper part of the filter, at different instants of time. The left image shows a dye jet flowing through the inlet connector. The jet is deflected and tends to flow in direction of the E plane. At the left image is possible to see that the jets flows in a clockwise sense and finally achieves the inlet connector. There is a blue spot near the central region of the filter. This spot shows a recirculating flow which difficults the convective mass transport and the dye dispersion.

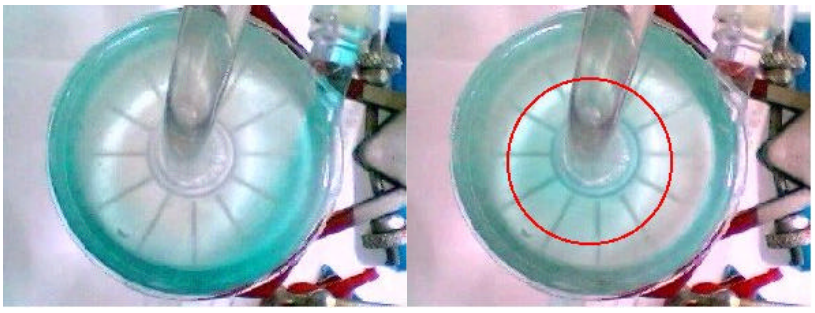

Fig. 8. Flow visualization at the upper part of the filter at two different instants of time

Flow visualization at planes E, SE, S and SO is show at figure 9, respectively. At planes E and SE dye flows in a descending clockwise sense, showing that the velocity vector has at least two components, the tangential and axial. At planes S and SO the axial component vanishes and the dye flows horizontally.

Fig. 9. Flow visualization at planes E, SE, S and SO, respectively

Figure 10 shows the flow visualization at planes O, NO, N and NE, respectively. At planes O and NO the flow has an ascending behavior, this mean that the axial velocity has a positive value and the blood is not collected by the outlet channel. Dye flows vertically at plane N and this phenomenon will be explained combining the information from planes NO and NE. The visualization at plane NE shows the incoming jet being divided because part of the dye flows in a clockwise sense, in direction of plane E while part of it flows in direction of the N plane. The flow coming from the NE plane will interact with the flow coming from the NO plane and this fact combined with low pressure area created by the presence of the incoming jet, near the plane NO where the inlet connector is present, explains the flow behavior at plane N.

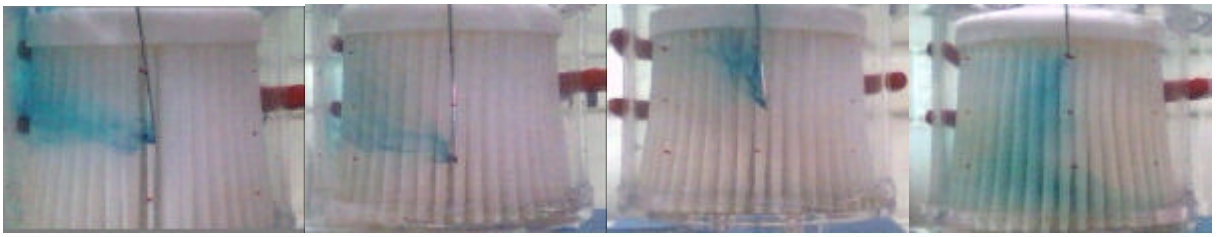

Fig. 10. Flow visualisation at planes O, NO, N and NE, respectively

3.1 LDA Measurements

Figure 11 shows the tangential velocity isocurves at the four planes. The velocity has a maximum value, absolute value, of 0,58 m/s at plane E which decreases until 0,18 m/s at plane N. In all planes the velocity decreases radially, it presents a maximum value near the wall which decreases near the filtering element.

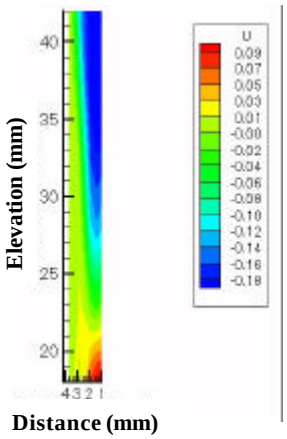

Plane N

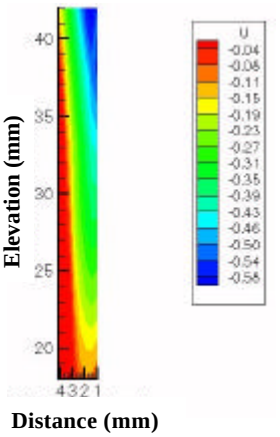

Plane E

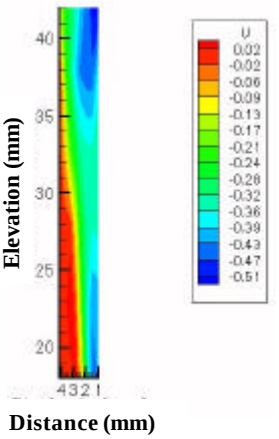

Plane S

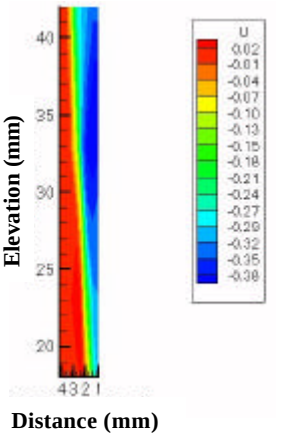

Plane O

Fig. 11. Tangential velocities (m/s) at the four planes

At the plane O the velocity increases with the elevation decreasing. In all planes is possible to see a reversal flow at region near the filtering element, because the velocity is negative near the wall and positive near the polyester. In figure 12 is possible to see the axial velocity at the four planes. At the plane N the component is positive indicating an ascending flow and negative meaning a descending flow. The flow has a descend behavior in plane E because the velocity is negative. At plane S the flow is descend near the wall and ascending near the filtering element indicating a reversal flow in this plane. Is also possible to see a reversal flow at plane O.

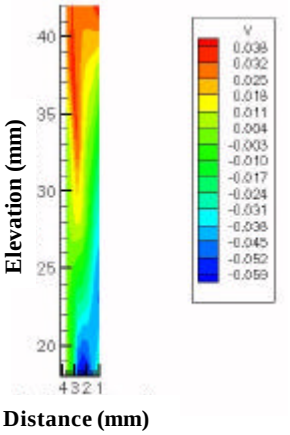

Plane N

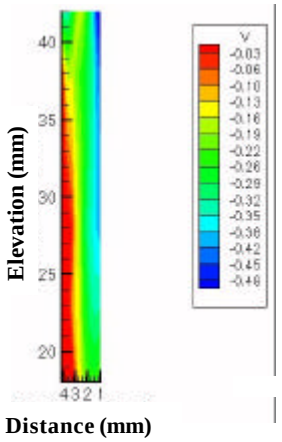

Plane E

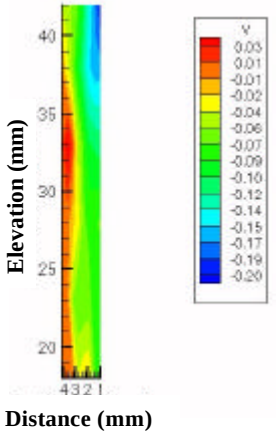

Plane S

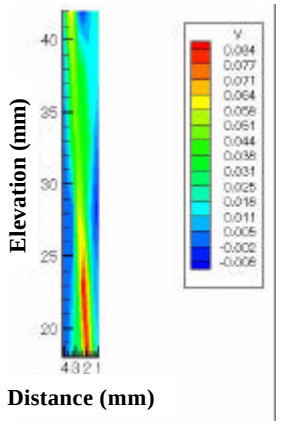

Plane O

Fig. 12. Axial velocities (m/s) at the four planes

Figures 13 and 14 show the turbulent kinetic energy at the four planes. It has a maximum value in plane E due to the proximity of the point where the incoming jet changes flow direction. The presence of the jet can be observed at plane S because in this plane the turbulent kinetic energy has a maximum value of 9.23E-03 m^2/s^2 at 42 mm. At planes N and O the turbulent kinetic energy decreases showing that mostly of the jet energy is transferred to the flow at planes E and S.

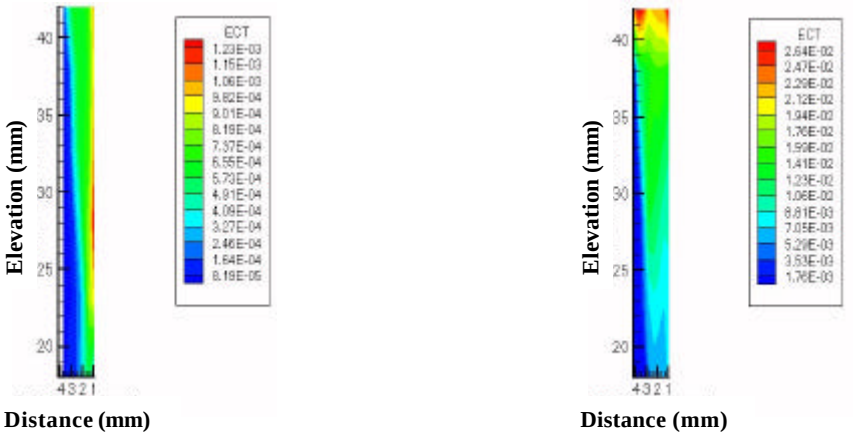

Fig. 13. Turbulent kinetic energy (m^2/s^2) at planes N and E, respectively.

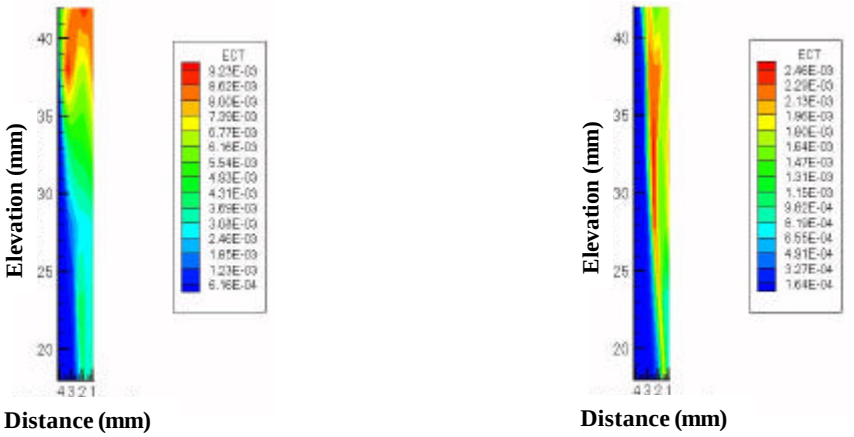

Fig. 14. Turbulent kinetic energy (m^2/s^2) at planes S and O, respectively.

The turbulent shear stress distribution in the four planes is shown in figure 15. At the plane N the shear stress decreases radially. In planes S and O the shear stress has a maximum value at the central part of the inlet channel and decreases near the wall and filtering element. In the plane E the stress is maximum at the higher elevation, as the turbulent kinetic energy, due to the presence of the jet. The maximum value observed was 32.25 Pa at the plane E.

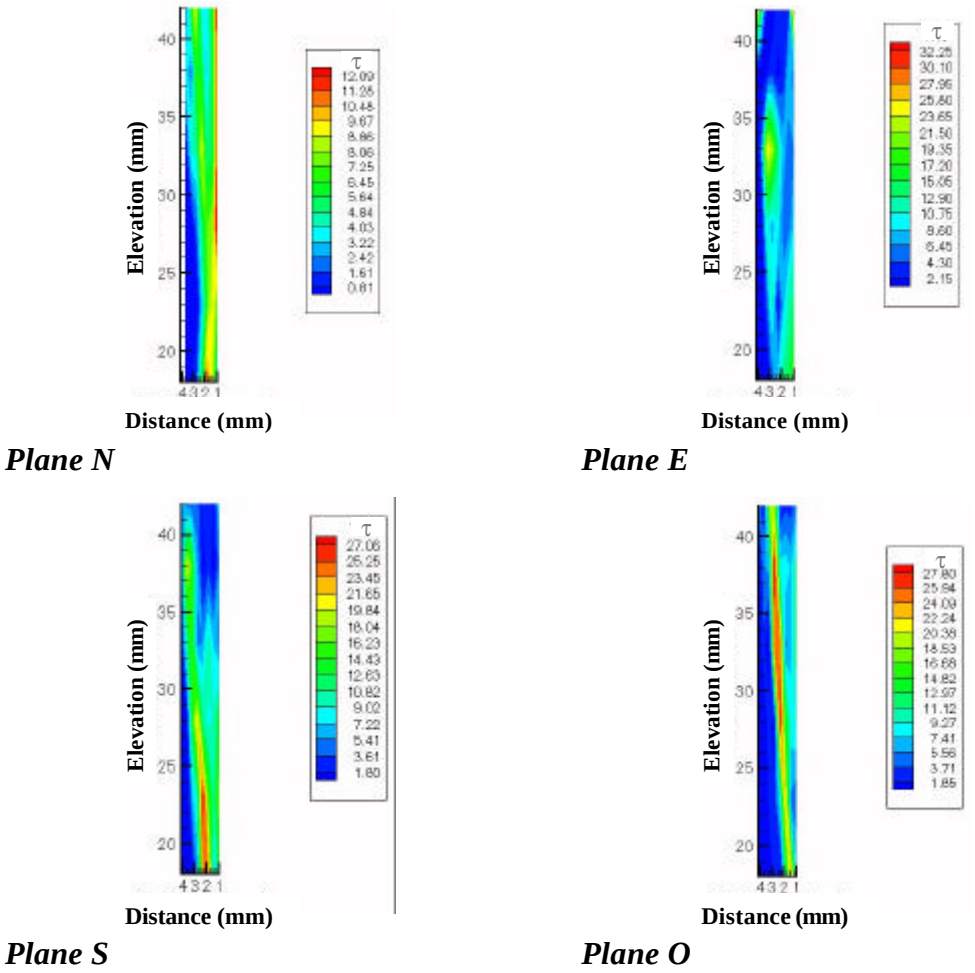

Fig. 15. Turbulent shear stress (Pa) at the four planes

4. SUMMARY

This work reports the use of laser Doppler velocimetry to study the flow inside an arterial blood filter. A test bench was developed in order to allow the use of a LDA system and a working fluid with viscosity and density similar those of blood was used. Velocities profiles and their fluctuations were measured at four planes and results show that the flow structure is influenced by the incoming flow in the filter. Velocity fluctuations were used to evaluate turbulent shear stresses. Results show also this filter has a low tendency to damage red blood cells, considering the measured planes. The flow was visualised using the dye injection technique and the results are in agreement with the LDA measurements.

ACKNOWLEDGEMENT

This work was financed by CNPq (Brazilian research council), grants n°200729/95-0 and n°300556/97-7. The contribution of S. Evangelisti to the LDA measurements and V. Ponzio to the construction of the experimental setup is gratefully acknowledged.

REFERENCES

Baldwin, J.T., Deutsch, S., Petrie, H.L. & Tarbell, J.M. (1993). "Determination of principal Reynolds stresses in pulsatile flows after elliptical filtering of discrete velocity measurements". Journal of Biomechanical Engineering, 115, p.396-403.

Dybbs, A, and Edwards, R.V. (1987). “Refractive index matching for difficult situations”. Laser anemometry advances and applications.

Higdon, A.,Ohlsen, E.H., Stiles, W.B., Weese, J.A. and Riley, W.F. (1985). “Mechanics of Materials”. New York, NY : John Wiley & Sons.

Paul, R., Schügner, F., Reul, H., Rau, G., (1999), “Recent findings on flow induced blood damage : critical shear stresses and exposure times obtained with a high shear Couette-system”, Artificial Organs, 23, n.7, p.680.

Rand, R.P. (1964). “Mechanical properties of red cell membrane. Part 2, Viscoelastic breakdown of the membrane”, Biophysics, 4, p.303-316.

Sallam, A.M., Hwang, N.H.C. (1984). “Human red blood cell hemolysis in a turbulent shear flow : contribution of Reynolds shear stresses”, Biorheology, 21, p.783-797.

Sutera, S.P. (1977). “Flow induced trauma to blood cells”, Circulation research, 41, n.1, p.2-8.

Sutera, S.P., Mehrjardi, M.H. (1975). “Deformation and fragmentation of human red blood cells in turbulent shear flow”, Biophysical journal, 15, p. 1-10.

Waaben, J., Sørensen, H.R., Andersen, U.L.S., Gefke, K., Lund, J., Aggestrup, S., Husum, B., Laursen, H., Gjedde, A. (1994).“Arterial line filtration protects brain microcirculation during cardiopulmonary bypass in the pig”, The journal of Thoracic and Cardiovascular Surgery, 107, n.4, p. 1030-1035.

Wurzinger, L.J., Opitz, R., Blasberg, P. e Schönbein, S. (1985). “Platelet an coagulation parameters following millisecond exposure to laminar shear stress”. Thrombosis and Haemostasis, 54, n.2, p.381-386.